Some characteristics of an interior explosion within a room without venting

V.R. Feldgun[a], Y.S. Karinski* and D.Z. Yankelevsky[b]

National Building Research Institute, Technion-IIT, Haifa, Israel

Abstract. The paper presents a study aimed at understanding some characteristics of an interior explosion within a room with limited or no venting. The explosion may occur in ammunition storage or result from a terrorist action or from a warhead that had penetrated into this room. The study includes numerical simulations of the problem and analytical derivations. Different types of analysis (1-D, 2-D and 3-D analysis) were performed for a room with rigid walls and the results were analyzed. For the 3D problem the effect of the charge size and its location within the room was investigated and a new insight regarding the pressure distribution on the interior wall as function of these parameters has been gained. The numerical analyses were carried out using the Eulerian multi-material approach. Further, an approximate analytical formula to predict the residual internal pressure was developed. The formula is based on the conservation law of total energy and its implementation yields very good agreement with the results obtained numerically using the complete statement of the problem for a wide range of explosive weights and room sizes that is expressed through a non-dimensional parameter. This new formula is superior to existing literature recommendations and compares considerably better with the above numerical results.

Keywords: confined explosion; shock wave; wave reflection; peak pressure; residual pressure.

1. Introduction

Confined explosions may occur due to various reasons and their effect may be very severe and may lead to the structure's collapse (Griffiths *et al.* 1968). The damage caused by a confined explosion is more severe than that of a similar external explosion. The resulting damage depends on the geometrical parameters of the confined space where the explosion occurs (geometrical sizes, the charge location, the openings' existing and their size etc.), the structural and material characteristics of the room's elements and the charge's type and size.

The end goal of an analysis of a confined explosion is to predict the immediate local damages caused by the explosion. These damages occur shortly after the shock waves arrival at the structural components and their damage may lead to further damage and even collapse of the entire structure (Dorn *et al.* 1996, Luccioni *et al.* 2005). This analysis includes both the complex pressure

---

*Corresponding author, Senior Researcher, E-mail: karinski@technion.ac.il
[a]Senior Researcher, E-mail: aefeldgo@techunix.technion.ac.il
[b]Professor, E-mail: davidyri@technion.ac.il

propagation and distribution on the interior boundaries of the room at all times and the dynamic response of the structural elements including the damage formation. Such an analysis may be performed either without coupling of the shock wave reflection and dynamic pressure distribution and the elements' structural dynamic response (O'Daniel and Krauthammer 1997) or with coupling (Chock and Kapania 2001, Vaidogas and Egidijus 2003, Corneliu 2004).

To predict the contact dynamic pressure acting on the interior of the room's envelope structural elements (walls, ceiling, floor, partitions etc.) one should consider the charge properties and location, the confining space geometry, the presence of openings on the envelope elements etc. This analysis is based on the shock wave interactions with the room boundaries. This is a well known problem that has been studied in many books (Baker *et al.* 1983, Kinney 1962, Bangash 1993), handbooks and reports (A718300 1974, Ben-Dor 2000), reports (Michael and Swisdak 1975) and manuals (TM-5-855-1 1986, AASTP-1 2006). The simplest problem of the explosion shock wave-structure interaction deals with the external explosion in the proximity of an obstacle (Shear and Makino 1967, Liang *et al.* 2002, Podlubnyi and Fonarev 1974, Kivity 1992, Igra *et al.* 2003). The problem of a confined explosion is considerably more complicated and less investigated. This paper is devoted to study and enhance the understanding of some characteristics of an interior explosion within a room with limited or no venting.

2. Typical simulations of blast loads

The time history of a blast pressure acting on a boundary wall resulting from a fully or a partially confined internal explosion is complex mainly due to the repetitive shock waves reflections from the closed space faces (walls, ceiling, and floor). Fig. 1 shows a typical time history of the contact pressure and impulse due to an external explosion (Eamon 2007). One can see that the contact pressure is characterized by a sharp increase of a peak pressure after which a quick decay occurs. The pressure rapidly drops to zero.

In the case of an internal explosion the blast pressure time history is considerably more complex. Even in a one-dimensional problem (a spherical or a cylindrical charges inside a spherical or a
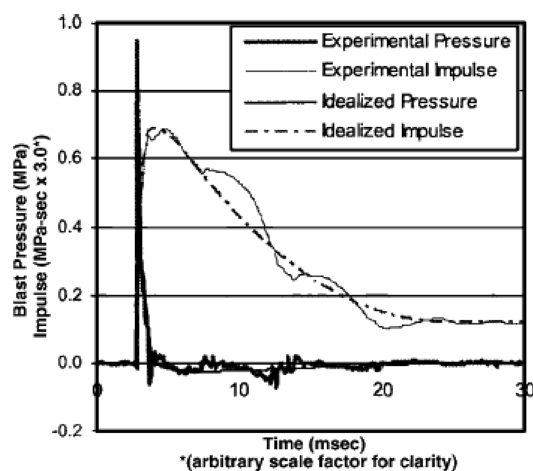

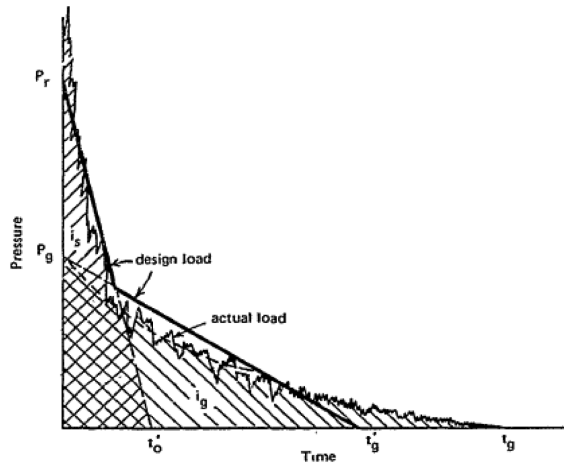Fig. 1 Blast wave pressure time history of an external explosion (Eamon 2007)

Fig. 2 Overpressure in the cube without ceiling (Keenan and Tancreto 1974)
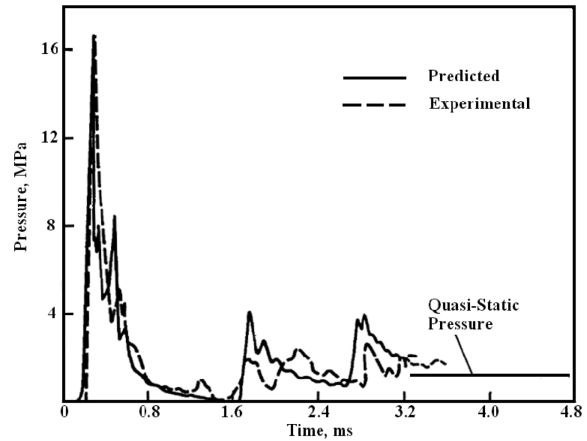

Fig. 3 Overpressure time history in a cylindrical vessel (Bangash 1993, Gregory 1976)

cylindrical vessel correspondingly), the contact pressure time history shows several peaks. For a fully confined space, the pressure time history converges to the constant permanent overpressure caused by pressure of explosive products and denoted as the gas pressure. For a partially confined explosion, where openings in the envelope allow the pressure release, the overpressure is diminishing to zero at a rate that depends on the relative openings area and on their locations. Figs. 2 and 3 show the typical overpressure time history for a partially confined (Fig. 2 - Keenan and Tancreto 1974) and a fully confined space (Fig. 3 - Bangash 1993, Gregory 1976).

The overpressure time histories of a partially confined space may also be observed in the case of an explosion occurring at a crossroad of an urban area in the proximity of surrounding tall buildings (Smith *et al.* 2001, Remennikov and Rose 2005, Smith and Rose 2006). Such problems are characterized by very quick overpressure decay with time. The first peak is always characterized by the highest peak pressure and the number of the following peaks is relatively limited.

On the contrary, in the case of a confined space with a relatively small openings area the pressure duration is relatively long and the number of after-peaks is relatively large.

The simplest problems of confined explosions are the one-dimensional problems of a spherical charge at the center of a spherical vessel or of a line-charge along the axis of a cylindrical vessel. For such relatively simple problems we may use simplified models to obtain analytical solutions for the vessel's walls response (Marchenko and Romanov 1984, Zhu *et al.* 1997, Auslender and Combescure 2000, Duffey and Romero 2003). In such simplified models the contact pressure or the impulse is predefined from empirical relationships (Alexsandrov *et al.* 1982, Tsypkin *et al.* 1982).

According to various sources, the first three peaks may be taken into account to describe the dynamic contact pressure after which a constant gas overpressure may describe the pressure acting on the inner envelope. For a line charge explosion placed along the axis of a cylindrical vessel (plane problem), an existing simplified analytical formula defines the first 3 pulses by a triangular shape (see Fig. 4) with peaks of decreasing magnitude by a factor of 0.5, i.e., the peak magnitude equals to half the magnitude of the preceding peak (Baker *et al.* 1983, Bangash and Bangash 2006). The pulses durations are constant and equal to $T_R = 2t_a$, where t_a is the arrival time of the cylindrical incident shock wave to the cylindrical vessel's boundary and its magnitude depends on the
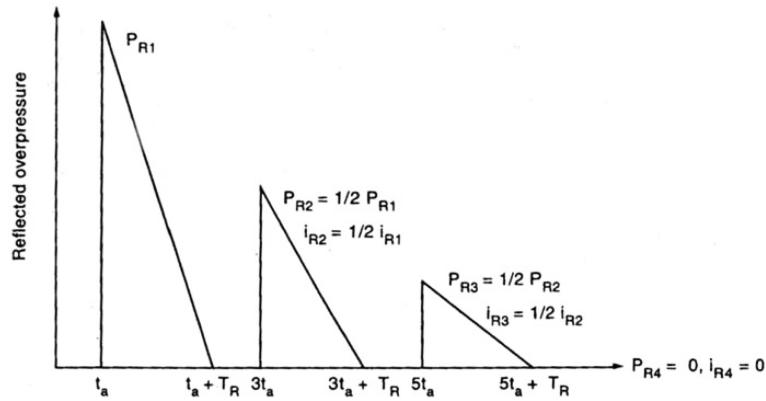
Fig. 4 Simplified (3-peaks) internal blast pressure (Baker *et al.* 1983, Bangash and Bangash 2006)

explosive material's type and on the vessel's radius. It turns out that the impulse magnitude of each pulse is half the magnitude of the preceding pulse. Note that the existing literature does not consider the residual quasi-static overpressure that follows the dynamic blast action (see Fig. 3). The sources also do not specify how to evaluate the first peak P_{R1} which is obviously also dependent on the explosive material's type and on the vessel's radius.

3. The effect of number of peaks on the response of a flexible shell

Consider a one dimensional problem of the dynamic response of a cylindrical elastic shell, of radius R and thickness h, to the internal pressure $P(t)$ that is described in Fig. 4.

The equation of motion has the following form

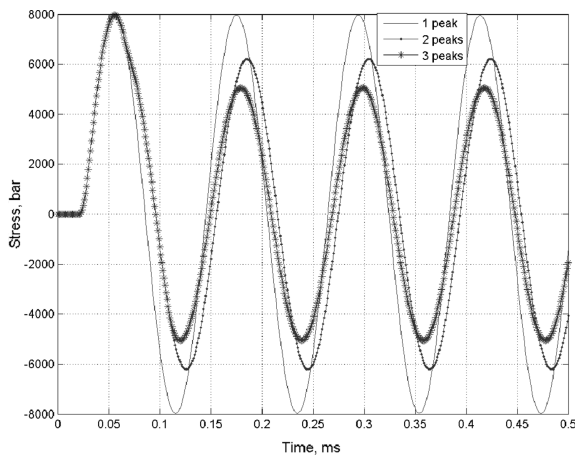$$\frac{d^2u}{dt^2} + \frac{1}{\rho_0}\frac{\sigma}{R} = \frac{P(t)}{\rho_0 h} \tag{1}$$

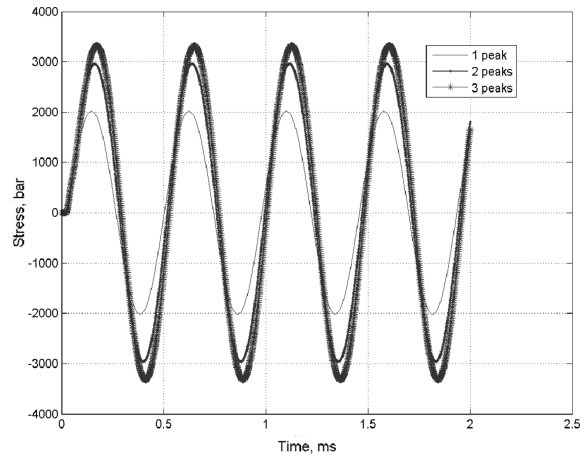Fig. 5 Stiff shell hoop stress time history ($T_1 = 0.119$ ms)

Fig. 6 Flexible shell hoop stress time history ($T_2 = 0.477$ ms)

Where

$$\sigma = \frac{E}{1 - \mu^2} \frac{u}{R} \tag{2}$$

Here u is the shell median surface's displacement, σ is the hoop stress, E, μ, ρ_0 are the respective values of the shell's Young's modulus, Poisson's ratio and density. The calculations were performed for two values of Young's modulus: $E_1 = 2.0 \times 10^6$ bar and $E_2 = E_1/16$ and for the following other parameters: $\mu = 0.29$, $\rho_0 = 7.88$ g/cm^3, $h = 0.5$ cm, $R = 10$ cm. The pulse load action of one- two- and three- impulses have been studied, where the first pulse parameters (Fig. 4) are the following: $t_A = 0.021$ ms; $T_R = 0.014$ ms; $P_{R1} = 1200.0$ bar. The following pulse peak (if it exists) is equal to half of the previous peak's value and the peaks durations are equal to each other. Depending on the Young's modulus values, the corresponding shells natural periods are $T_1 = 0.119$ ms and $T_2 = T_1 \times 4 = 0.477$ ms. Figs. 5 and 6 describe the hoop stress time history depending on the number of pulses. One can see that for the stiffer shell (E_1, T_1 – Fig. 5) the additional peaks decrease the stress amplitude while for the flexible shell (E_2, T_2 – Fig. 6) they increase the amplitude.

Therefore, the number of peaks acting on the shell wall significantly affect the shell's response and this effect qualitatively and quantitatively depends on the shell's natural period.

4. The effect of the shell's flexibility on the contact pressure due to a confined explosion

In general, the blast response of the structure's walls affect the contact pressure, and a coupled analysis is then required. When the structural elements are relatively rigid, their motion does not affect the blast pressure magnitude and the analysis maybe uncoupled. To examine the effect of the structure's flexibility on its dynamic response due to a confined explosion, the problem of a symmetrical TNT line charge explosion inside two cylindrical vessels (of radii $R = 40$ cm and $R = 10$ cm) were analyzed. The analysis was performed with AUTODYN-11. The analysis was performed for a rigid wall vessel as well as for an elastic plastic shell having the thickness $h = 0.5$ cm
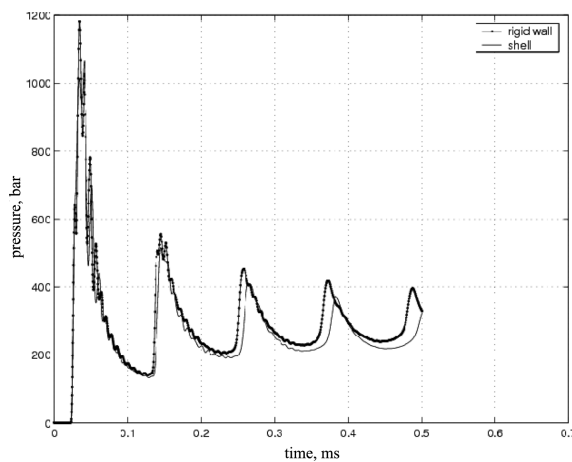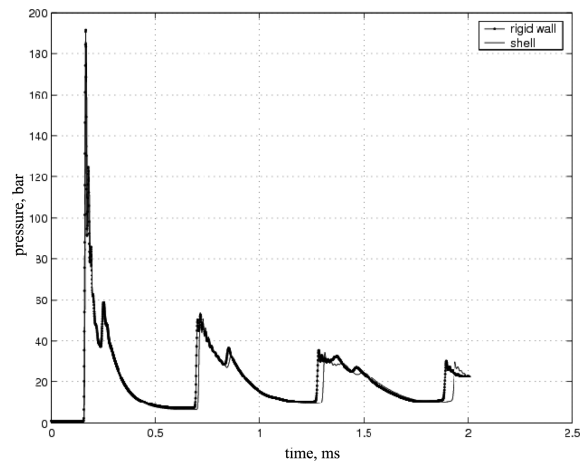

Fig. 7 $R = 10$ cm   Fig. 8 $R = 40$ cm

and the following physical properties: Young's modulus $E = 2.0 \times 10^6$ bar, Poisson's ratio $\mu = 0.29$, an ultimate hoop stress $\sigma_Y = 5000$ bar, a plastic hardening modulus $g = 2830$ bar, and density $\rho_0 = 7.88$ g/cm^3.

Figs. 7, 8 show a comparison of the contact pressure for a rigid and for flexible vessels.

One can see that the effect of the vessel's flexibility within this range on the contact pressure due to a confined explosion is minor and the uncoupling of the blast pressure calculation and structure's response analysis may be applied in the examined cases. Obviously with a considerably smaller vessel's thickness a stronger interaction is expected and the coupled analysis may be unavoidable.

5. The plane analysis of a confined explosion

This section presents a number of plane simulations of reflected (blast) waves as an initial approximation of blast response of a rectangular room structure with plane wall panels. The contact pressure has been calculated at the centre of rigid wall as well as at the room corner for both free and partially or fully confined explosions.

5.1 The effect of walls locations on the contact pressure due to a nearby explosion

Two following simulations are performed to examine the effect of an obstacle (floor) that is placed perpendicularly to a given rigid wall, on the contact blast pressure. In the first problem we study the pressure time history acting on a single wall due to a nearby explosion of the TNT line charge (the wall-charge distance is equal to five radii of the charge R_0). The second simulation deals with the same charge explosion in proximity to the wall-floor corner while the charge is located at a distance h from the floor (Fig. 9).

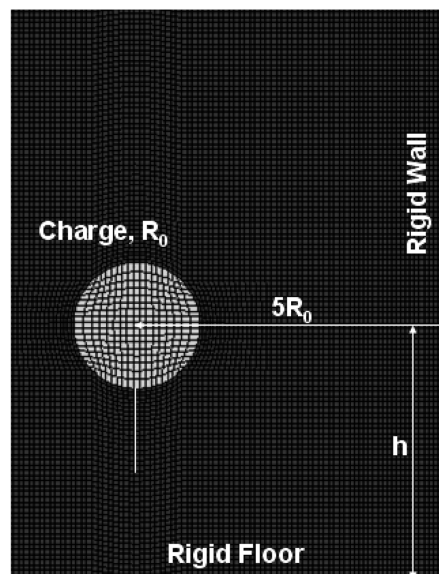In both cases the pressure was calculated with respect to the wall point at shortest distance from

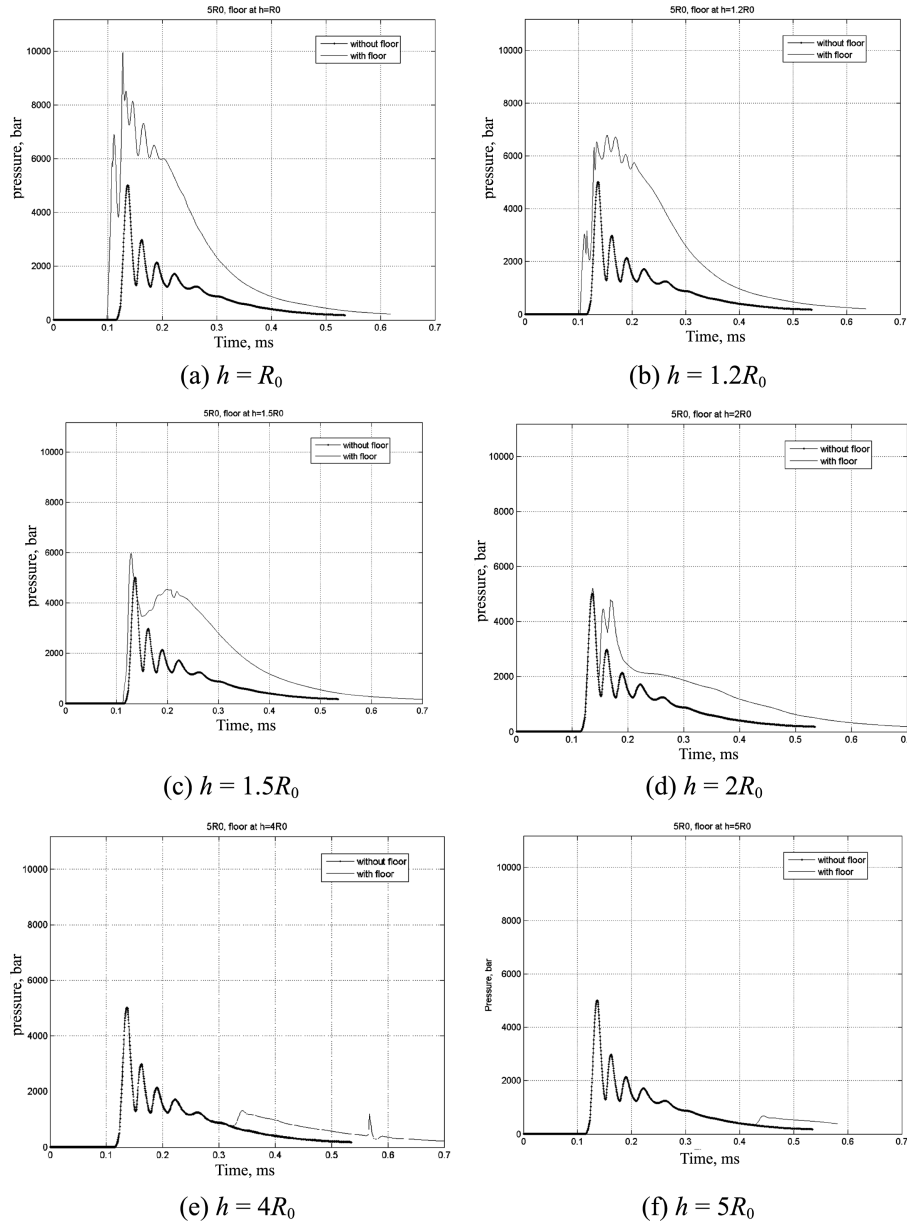Fig. 9 Charge explosion in the proximity to the wall-floor corner

(a) $h = R_0$ (b) $h = 1.2R_0$

(c) $h = 1.5R_0$ (d) $h = 2R_0$

(e) $h = 4R_0$ (f) $h = 5R_0$

Fig. 10 Contact pressure time histories

the charge. Figs. 10(a)-(f) show comparisons for various floor distances h.

One can see that for the case when the charge is close to the floor (Figs. 10(a)-(b)), the rigid floor produces a fore-shock preceding the peak pressure. The fore-shock is sometimes larger than the peak blast pressure that develops in absence of the floor. When the distance h increases, the fore-shock disappears and the peak pressures for both cases becomes similar while and the after-peaks are different (Figs. 10(c)-(d)) and this difference decreases when h further increases. For a relatively large distance from the floor ($h > 4R_0$) the calculated signals are about the same (Figs. 10(e)-(f)).

5.2 Fully and partially confined explosions

Consider the explosion of TNT charge at the centre of 2D 300 × 300 cm space. The room size corresponds to a meshing of 69 × 69 × 69 cells for. The charge size is determined from 5 × 5 cells (21.7 × 21.7 cm) that represent an explosive mass equivalent to about 16 kg cubical charge (see section 6). This model will allow us to examine the effect of the degree of venting (Fig. 11). The calculations were performed for one- two- three- and four-walls confining the space. Figs. 12(a)-(e) show the time histories of the pressure at the left hand side wall centre for all these cases.
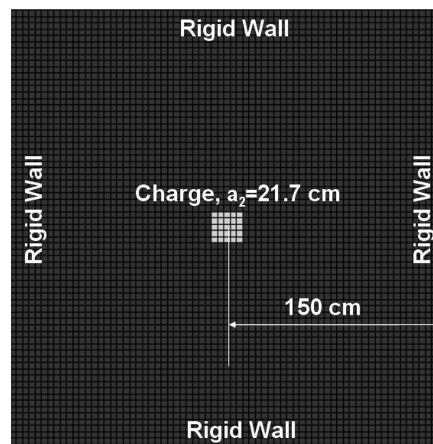

Fig. 11 The effect of the degree of space (room) closure

(a) One wall

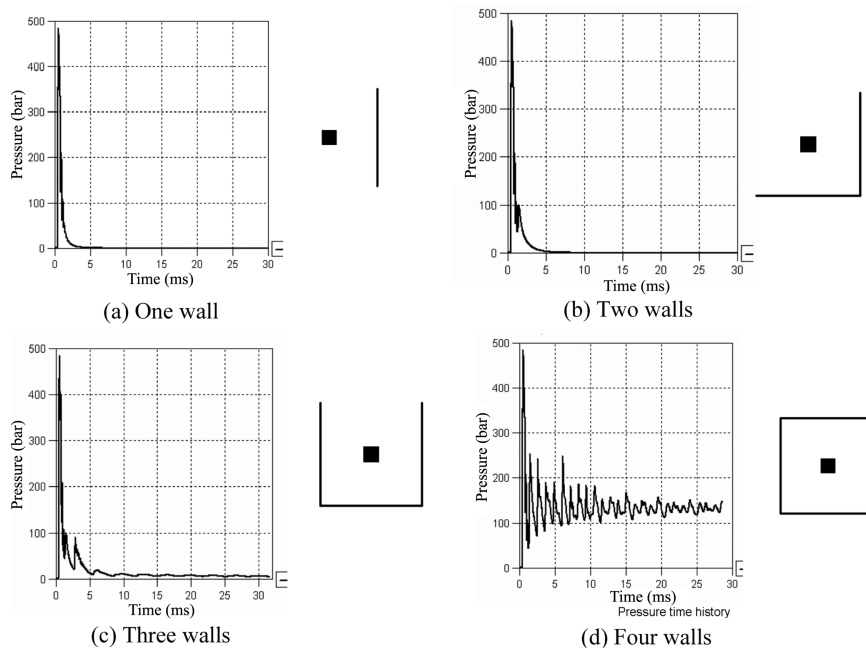(b) Two walls

(c) Three walls

(d) Four walls

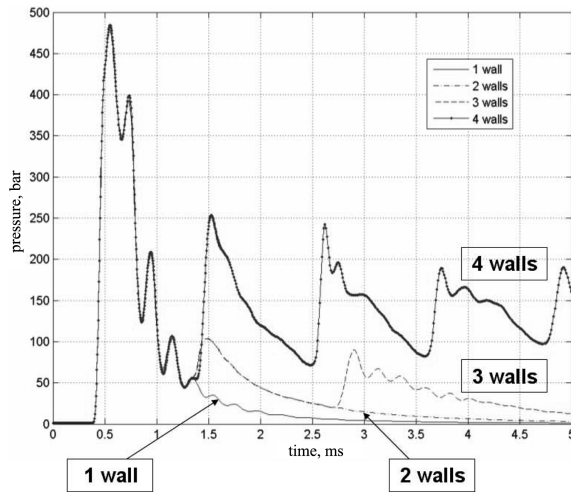Fig. 12 Contact pressure at the wall centre
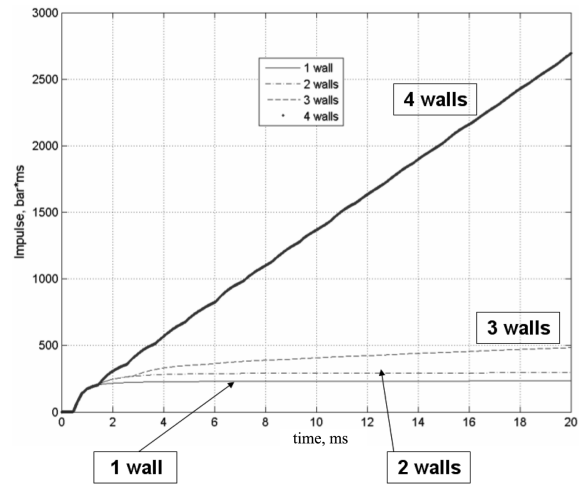
Fig. 13 Pressure time history

Fig. 14 Impulse time history

On the contrary, to sub-section 5.1 this explosion is relatively distant from the walls (about 7 charge radii-Fig. 10(f)). All the above cases yield about the same first peak (about 500 bar) but the following peaks are different, especially for the case of a fully confined room (Fig. 12(d)) as compared with all the other cases (Figs. 12(a)-(c)). Fig. 13 demonstrates this comparison for the early time ($t \leq 5$ msec). The difference of the after-peaks yields a significant difference of the impulse $I(t) = \int_0^p p(\tau) d\tau$ - as shown in Fig. 14.

6. 3D analysis

A three dimensional problem is examined, with a cubicle $21.7 \times 21.7 \times 21.7$ cm TNT explosive placed at the centre of $300 \times 300 \times 300$ cm cubicle room without openings (fully confined explosion). The room's walls are assumed to be rigid (Fig. 15).
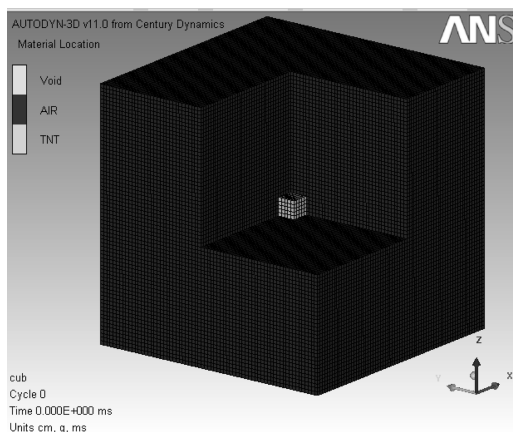

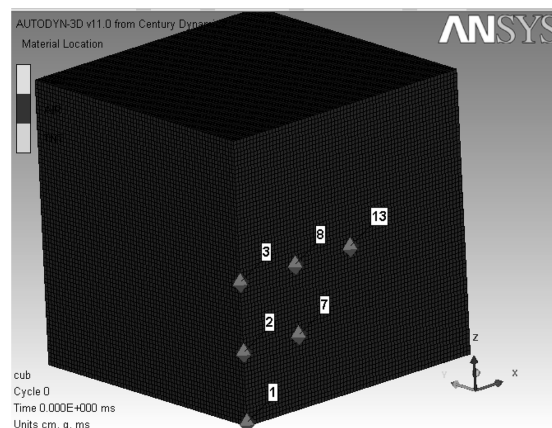Fig. 15 3D-analysis-problem description

Fig. 16 3D analysis-the gauges

6.1 The contact pressure distribution

The calculations were performed using AUTODYN-11. The program calculated the contact pressure at the following points (see gauges position in Fig. 16): 1 – the room corner, 2 – the edge quarter, 3 – the edge mid-point, 7 – the diagonal quarter, 8 – the wall mid-line quarter, 13 – the wall centre.

(a) The room corner

(b) The edge quarter

(c) The edge mid-point

(d) The diagonal quarter

(e) The wall mid-line quarter

(f) The wall centre

Fig. 17 Contact pressure at the room wall

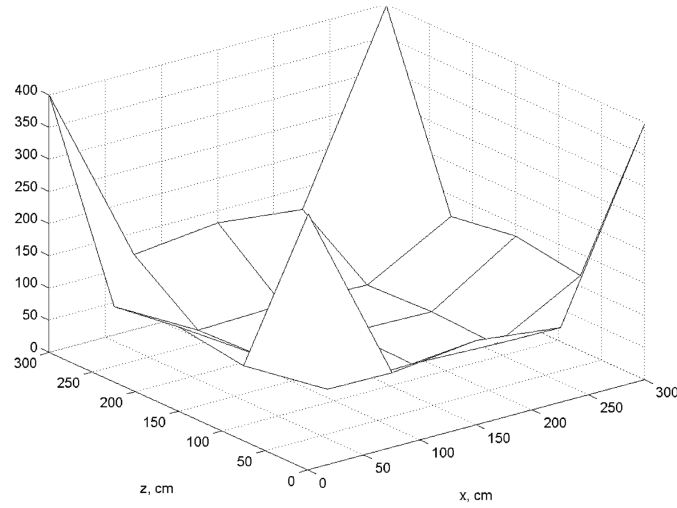Fig. 18 Peak pressure envelope

(a) $t = 0.65$ msec

(b) $t = 0.7534$ msec

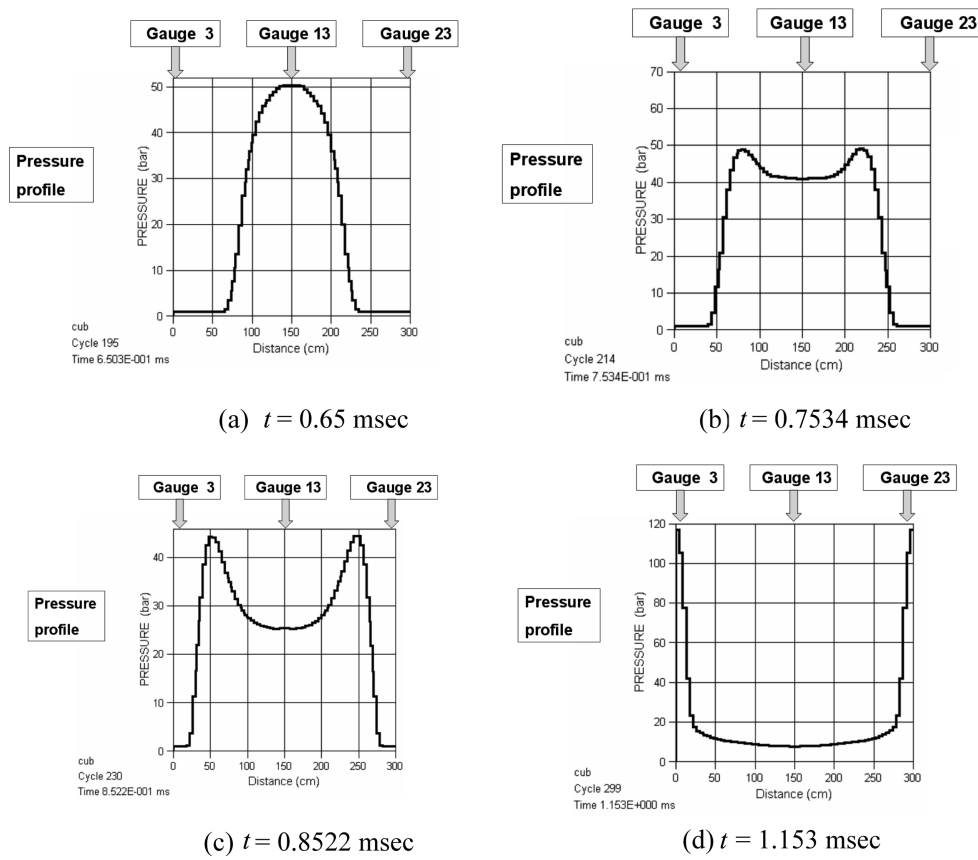(c) $t = 0.8522$ msec

(d) $t = 1.153$ msec

Fig. 19 Pressure distribution along the wall mid-line

Figs. 17(a)-(f) present the contact pressure's time history for these points.

One can see that for the given charge size, the maximum value of peak pressure (about 400 bar) is developed at the room corner (gauge 1) – see Fig. 17(a). The minimum pressure magnitude (less than 50 bar) was calculated at the gauge 7 (Fig. 17(d)) that is located at the diagonal quarter. Fig. 18 shows the peak pressures envelope over the entire wall.

Note that the peak pressure values at various points of Fig. 18 appear at various instances; hence Fig. 18 does not describe a certain pressure distribution but an envelope. Figs. 19(a)-(d) show the pressure distribution along the wall mid-line at various instants (gauge 23 is placed on a parallel edge mid-point symmetrically to gauge 3 – see Fig. 16).

One can see that at the beginning of the process the peak pressure is developed at the wall centre (Fig. 19(a)). Then after it moves to the edge's direction (Figs. 19(b)-(c)). During this process, the pressure at the central point decreases when the peak pressure increases. These figures demonstrate that the common simplified assumption that the wall's response may be analyzed assuming a uniform dynamic pressure distribution is incorrect.

6.2 The effect of the charge size

The analysis of the previous sub-section was performed for a relatively small charge in comparison to the room size. When the charge's dimensions increase, the peak pressure's envelopment (Fig. 19(a)) shape is changed and its maximum may appear at the wall centre. Fig. 20 shows the relationship between the peak pressure at the room corner (max value at gauge 1) to its maximum value at the wall centre (gauge 13) depending on the relative charge size (a/A) ($A = 300$ cm is the cubicle room side length and "a" is the cubicle charge's dimension).

For a relatively small charge, the peak pressure at the corner is larger than at at the center and this ratio increases while $a/A < 0.1$ (the maximum ratio is about 10.5 – Fig. 20). Upon further increase of the ratio a/A, the ratio of the maximum pressures decreases. For $a/A = 0.4$ the peak pressures at the corner and at the wall centre are equal. For even larger charges the maximum peak pressure
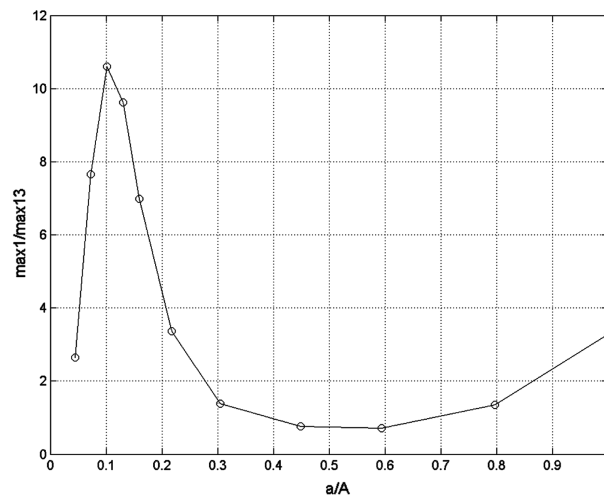

Fig. 20 The normalized peak pressure at the room corner to its magnitude at the wall centre depending on the relative charge size
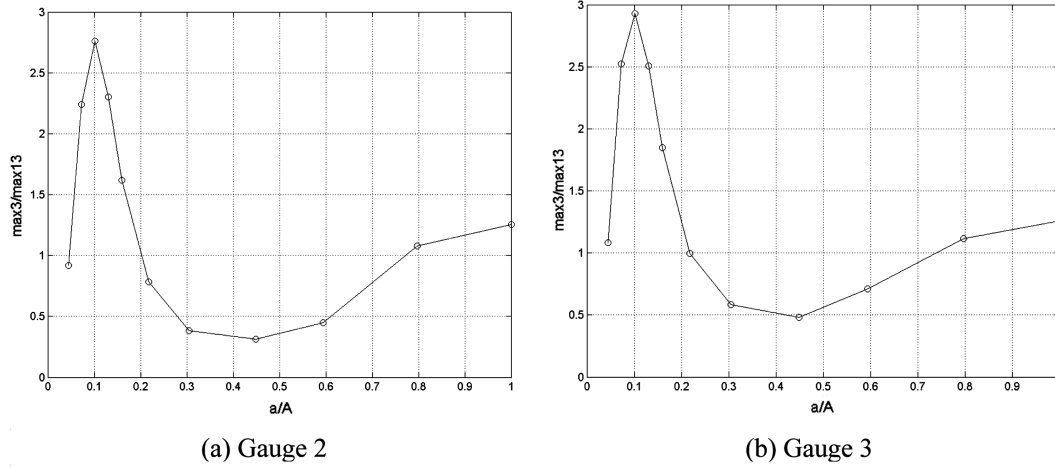
(a) Gauge 2   (b) Gauge 3

Fig. 21 The normalized peak pressure

develops at the wall centre (as long as *a/A* < 0.8). Note that for large *a/A* the problem becomes unreal, as we deal with a very large explosive quantity that produces enormous pressures. A similar problem of large *a/A* may appear in the case of gas explosion, however in that case another model is required to represent the equation of state of the gas and its energetic properties.

Figs. 21(a)-(b) show that a similar relationship for the pressures ratio (with respect to the maximum pressure at the wall center-gauge 13) as function of *a/A* appears for an edge quarter gauge (gage 2) and for the mid-point gauge (gage 3). In both cases the maximum pressure ratio is about 3.

7. The residual overpressure for a confined explosion

In this section we shall develop a new analytical expression to evaluate the residual quasi-static gas pressure that is developed in the explosion process and remains for a rather long time within the fully confined space.

Consider the problem of charge of a volume V that explodes within a fully confined space of a volume V. The conservation of energy law may be written as follows

$$\frac{p_0}{\rho_0(\gamma_0-1)}\rho_0(V-v) + Q\rho_E v = \frac{p}{(\gamma-1)\rho}\rho V \tag{3}$$

Where ρ_E, ρ_0 are the explosive and initial air densities, γ, γ_0 are the adiabatic indexes of the air-explosive gas mixture and of the instant air, Q is the explosive specific heat of a constant volume. The first and second terms on the left-hand side of Eq. (3) express the internal energy of the air space excluding the charge and the internal energy of the explosive material respectively. The right-hand side presents the energy of the air-explosive gas mixture after the occurrence of the explosion and the wave process stabilization (quasi-statics). Eq. (3) yields the following expression for the residual pressure after the occurrence of a confined explosion
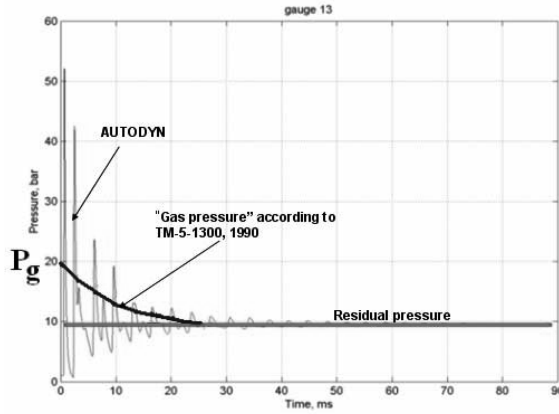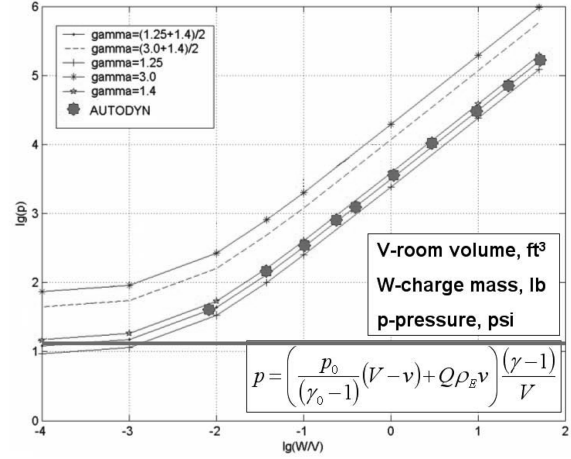
Fig. 22 Pressure at the rigid wall centre

Fig. 23 The residual pressure as function of W/V for various values of γ

$$p = \left(\frac{p_0}{(\gamma_0 - 1)}(V - v) + Q\rho_E v\right)\frac{(\gamma - 1)}{V} \qquad (4)$$

Note that Eq. (4) represents the full pressure; to obtain the residual overpressure one should subtract the initial air pressure p_0 from the right-hand side.

Fig. 22 presents the contact pressure at the rigid wall centre due to an explosion of a $21.7 \times 21.7 \times 21.7$ cm TNT charge that explodes at the centre of a $300 \times 300 \times 300$ cm cubical room without openings (see Figs. 14, 15). The system's parameters are the following: $\rho_0 = 1.225$ kg/m^3, $\rho_E = 1600$ kg/m^3, $p_0 = 10^5$ Pa, $\gamma_0 = 1.4$, $Q = 4.1868 \times 10^6$ J/kg. The adiabatic index of the air-explosive gas mixture γ is equal to the average of γ_0 and of the explosive gas adiabatic index for low-pressure (up to 1000 bar) is $\gamma_1 = 1.25$.

The red line indicates the residual pressure according to Eq. (4). One can see the good correspondence between the calculated results with the AUTODYN software and the analytical prediction with Eq. (4). The blue line shows the "gas pressure" P_g that appears in literature (TM-5-1300 1990) and the average pressure decrease with time. For a relatively stable process ($t > 20$ msec) these values (TM-5-1300 and prediction (4)) are similar.

The residual pressure (4) depends on the adiabatic indexes of the air-explosive gas mixture that is unknown. It depends on the amount of explosive material as well as on the final pressure, because the explosive materials adiabatic index γ_1 varies from 1.25 for the relatively low pressures (the order of 10^3 bar) to 3 for the high pressure range (the order of 10^5 bar). Fig. 23 demonstrates the dependence of a residual pressure (psi) on the parameter W/V (lb/ft^3) for various values of γ.

The red points indicate the results that were obtained from AUTODYN simulations and the red line indicates the atmospheric pressure. The most right point corresponds to the case when the explosives fills 80% of the room volume. Even in this case the residual pressure reaches about 700 bar and therefore, at the quasi-static state, the system is subjected to a relatively low overpressure. Now it is clear that the explosive materials' adiabatic indexes $\gamma = 3$ and $\gamma = (3 + 1.4)/2$ are not valid and its usage yields improper results (see two upper lines in Fig. 23). For a relatively large charge (the side is larger that 0.13 m) the best correspondence between the numerical results and analytical predictions (4) is obtained for $\gamma = 0.5(\gamma_0 + \gamma_1)$, ($\gamma_1 = 1.25$). When the charge is relatively
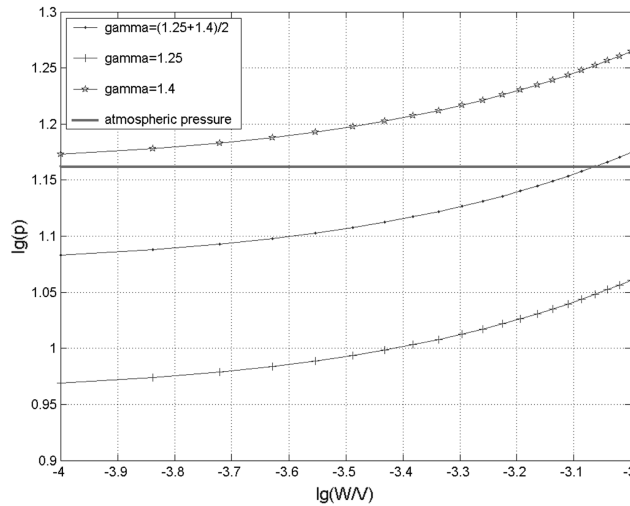
Fig. 24 The residual pressure for small weight charges for various values of γ

small, the effect of the explosive materials is small and $\gamma = \gamma_0$. Furthermore, Fig. 23 shows that the usage of the average $0.5(\gamma_0 + \gamma_1)$ for small charges (left-side points) yields a residual pressure that is somewhat smaller than the atmospheric pressure that, essentially, is physically not sound (see Fig. 24).

8. Conclusions

The paper presents a study aimed at understanding some characteristics of an interior explosion within a room with limited or no venting. The effect of parameters of both space geometry and the charge on the blast contact pressure has been examined.

The study includes numerical simulations of the problem. The number of after-peaks characterizes the confined explosion. The paper studies the effect of the number of impulses (after peaks) on the flexible shell response depending on its stiffness. The analysis yields significant quantitative and qualitative effect of the after-peaks number as well as the shell natural frequencies on the process.

The effect of the wall's flexibility due to a confined explosion on the blast contact pressure due to a confined explosion in air has been investigated. It was shown that due to a relatively short time of the non-stationary process this effect is minor and the uncoupling of the blast pressure calculation and structure's response analysis may be applied in certain cases.

Different types of analysis (1-D, 2-D and 3-D analysis) have been performed for a room with rigid walls and the obtained results were examined. For the 2D problem, the effect of the corner between adjacent panels as well as of the degree of the space confinement (1, 2, 3, 4 walls) on the contact pressure was studied for a nearby explosion. The analysis shows that the pressure time history for the fully confined explosion is very complex and is significantly different from the pressure time history in the case of a partially confined space.

The 3D simulation deals with the blast contact pressure distribution along the wall at various instances due to a fully confined explosion. The effect of the charge size and its location within the

room has been investigated and a new insight with regard to the peak pressures envelope as function of these parameters has been obtained. When the charge is relatively small the maximum peak pressure appears at the room corner, while for a relatively large charge (consuming 40-60% of the room space) the maximum peak pressure develops at the wall center.

Further, an approximate analytical formula to predict the residual internal pressure has been developed. The formula is based on the total energy conservation law and shows very good agreement with the numerical results obtained by AUTODYN Commercial Software for a wide range of the relative charge/room size. The new relationship compares very well with the above numerical results and is considerably superior to existing recommendations in the literature.

Acknowledgements

References

A718300 (1974), "Engineering design handbook. explosions in air. part one", Army Materiel Command Alexandria, VA.

AASTP-1 (2006), "Manual of NATO safety principles for the storage of military ammunition and explosives", NATO International Staff – Defense Investment Division.

Aleksandrov, L.N., Ivanov, A.G., Mineev, V.N., Tsypkin, V.I. and Shitov, A.T. (1982), "Plastic deformation of spherical steel shells under internal blast loading", *J. Appl. Mech. Tech. Phys.*, **23**(6), 831-835.

Auslender, F.A. and Combescure, A. (2000), "Spherical elastic-plastic structures under internal explosion. Approximate analytical solutions and applications", *Eng. Struct.*, **22**, 984-992.

Baker, W.E., Cox, P.A., Westine, P.S., Kulesz, J.J. and Strehlow, R.A. (1983), *Explosion Hazards and Evaluation*, Elsevier, Amsterdam.

Bangash, M.Y.H. (1993), *Impact and Explosion. Analysis and Design*, Spon Press, Blackwell Scientific Publications, Oxford.

Bangash, M.Y.H. and Bangash, T. (2006), *Explosion-Resistant Buildings*, Springer.

Ben-Dor, G., Igra, O. and Elperin, T. (2000), *Handbook of Shock Waves,* Academic Press, Elsevier.

Chock, J.M.K. and Kapania, R.K. (2001), "Review of two methods for calculating explosive Air blast", *Shock Vib. Dig.*, **33**(2), 91-102.

Corneliu, B. (2004), "Evaluation and rehabilitation of a building affected by a gas explosion", *Prog. Sturct. Eng. Mat.,* **6**(3), 137-146.

Dorn, M., Nash, M., Anderson, G., Jones, N. and Brebbia, C.A. (1996), "The numerical prediction of the collapse of a complex brick building due to an internal explosion", *ASME Publications- PVP*, **351**, 359-364.

Duffey, T.A. and Romero, C. (2003), "Strain growth in spherical explosive chambers subjected to internal blast loading", *Int. J. Impact Eng.*, **28**(9), 967-983.

Eamon, C.D. (2007), "Reliability of concrete masonry unit walls subjected to explosive loads", *J. Struct. Eng.*, **133**(7), 935-944.

Gregory, F.H. (1976), "Analysis of the loading and response of a suppressive shield when subjected to an internal explosion", *Minutes of the Seventeenth Explosive Safety Seminar*, Denver, Colorado.

Griffiths, H., Pugsley, A. and Saunders, O. (1968), "Report of the Inquiry into the Collapse of Flats at Ronan Point, Canning Town", Her Majesty's Stationery Office, London.

Igra, O., Hu, G., Falcovitz, J. and Heilig, W. (2003), "Blast wave reflection from wedges", *J. Fluid. Eng.*, **125**(3), 510-519.

Keenan, W.A. and Tancreto, J.E. (1974), "Blast environment from fully and partially vented explosions in cubicles", Tech. Rep. 51-027, NCEL, Port-Hueneme, CA.

Kinney, G.F. (1962), *Explosive Shocks in Air,* The Macmillan Co., New York.

Kivity, Y. (1992), "The reflected impulse on a curved wall produced by a spherical explosion in air", *25th Explosives Safety Seminar*, Anaheim, CA.

Liang, S.M., Wang, J.S. and Chen, H. (2002), "Numerical study of spherical blast-wave propagation and reflection", *Shock Waves*, **12**(1), 59-68.

Luccioni, B.M., Ambrosini, R.D. and Danesi, R.F. (2005), "Failure of a reinforced concrete building under blast loads", *WIT Trans. Eng. Sci.*, **49**, 336-345.

Marchenko, A.I. and Romanov, G.S. (1984), "Numerical simulation of processes in a spherical combustion chamber", *J. Eng. Phys. Thermophys,* **47**(4), 1230-1234.

Michael, M. and Swisdak, Jr. (1975), "Explosion effects in air", Final Report, A445810.

O'Daniel, J.L. and Krauthammer, T. (1997), "Assessment of numerical simulation capabilities for medium-structure interaction systems under explosive loads", *Comput. Struct.*, **63**(5), 875-887.

Podlubnyi, V.V. and Fonarev, A.S. (1974), "Reflection of a spherical blast wave from a planar surface", *Fluid Dyn.*, **9**(6), 921-926.

Remennikov, A.M. and Rose, T.A. (2005), "Modeling blast loads on buildings in complex city geometries", *Comput. Struct.,* **83**(27), 2197-2205.

Shear, R.E. and Makino, R.C. (1967), "A non-linear shock wave reflection theory", Pentagon Report Number: 0549946.

Smith, P.D. and Rose, T.A. (2006), "Blast wave propagation in city streets - an overview", *Prog. Struct. Eng. Mater.*, **8**, 6-28.

Smith, P.D., Whalen, G.P., Feng, L.J. and Rose, T.A. (2001), "Blast loading on buildings from explosions in city streets", *Proc. Institut. Civil Eng. Struct. Build.*, **146**(1), 47-55.

TM-5-1500 (1990), "Structures to resist the effects of accidental explosions", Department of the Army, the NAVY and the Air Force, Washington, DC, USA.

TM-5-855-1 (1986), "Fundamentals of protective design for conventional weapons", Department of Army, Washington, DC, USA.

Tsypkin, V.A., Cheverikin, A.M., Ivanov, A.G., Novikov, S.A., Mineev, V.N. and Shitov, A.T. (1982), "Study of the Behavior of closed steel spherical shells with single-stage internal explosive loading", *Strength Mater.*, **14**(10), 1353-1359.

Vaidogas, E.R. (2003), "Pressure vessel explosions inside buildings: assessing damage using stochastic accident simulation", *Struct. Eng. Int.*, **13**(4), 249-253.

Zhu, W., Xue, H., Zhou, G. and Schleyer, G.K. (1997), "Dynamic response of cylindrical explosive chambers to internal blast loading produced by a concentrated charge", *Int. J. Impact Eng.*, **19**(9-10), 831-845.